

Design, Implementation and Measurement of 26.6 GHz Patch Antenna using MEMS Technology

M. Abdel-Aziz, H. Ghali, H. Ragaie, H. Haddara*

E. Larique**, B. Guillon** and P. Pons***

Electronics and Comm. Eng. Dept., Ain Shams Univ., Cairo - EGYPT

*MEMScAP – EGYPT, ** MEMScAP - FRANCE

*** LAAS/CNRS - FRANCE

Abstract

This paper presents a 26.6 GHz patch antenna using MEMS technology. In this technology, the patch is suspended over a thin dielectric layer (membrane), which is deposited on a high index silicon substrate. In addition, the silicon substrate is fully etched under the patch, creating an air cavity region of very low dielectric constant ($\epsilon_r \cong 1$). The antenna is directly fed using a microstrip line, and a CPW-microstrip transition is used for probe measurements of the antenna return loss. The design is performed using the 3D electromagnetic simulator HFSS[®]. The measured antenna return loss is -17dB at 26.6 GHz, and the bandwidth is 4.5%. The antenna has a radiation efficiency of 61.7% and directivity of 7.9dB. The measured antenna cross-polarization level is less than -20 dB in both the E- and H-planes.

I. Introduction

Microstrip antenna is a very common element in telecommunications and radar applications since it provides a wide variety of designs, either planar or conformal. In addition, microstrip antennas could be fed by various techniques, besides its advantage of being compact and suitable for antenna array designs [1]. Recently, System-on-Chip (SOC) concept has become more in focus, implying that all passive and active components being integrated over silicon. The major problem in integrating antenna over silicon is the high dielectric constant ($\epsilon_r=11.9$). This has the drawbacks of easily excited surface waves, lower bandwidth, and degraded radiation efficiency. Another issue is the losses caused by the silicon conductivity.

The first problem can be remedied by the use of a MEMS technology to remove the silicon substrate below the antenna, and consequently synthesize a locally low dielectric constant ($\epsilon_r=1$) region around the antenna [1]. The second problem is overcome by using a High Resistivity Silicon (HRS) substrate, where the losses due to the substrate conductivity are minimized, improving the antenna radiation efficiency. The idea of creating an air cavity underneath the antenna can take many forms. First, it is possible to synthesize a predetermined dielectric constant from 1 to 11.9 by partially etching the silicon underneath the patch antenna. This technique has been adopted in [1-3]. It is also possible to suspend the antenna over closely spaced holes in the substrate [4]. Another approach is to etch all silicon substrate and suspend the patch over a dielectric membrane, as in [5]. In the present case, a HRS substrate is used, which has been etched on the backside. The design procedure will be explained in the following sections, together with simulated and measured results.

* On Leave from Ain Shams University

II. Design Procedure

A. Process Description

The used MEMS technology is based on a stress compensated 1.4 μm membrane layer consisting of $\text{SiO}_2/\text{Si}_3\text{N}_4$ (0.8 $\mu\text{m}/0.6\mu\text{m}$) deposited on a HRS substrate, as shown in figure 1. After the membrane is deposited, the patch and its feeding network are patterned on the topside of the wafer using 2.5 μm gold electroplating technique. The HRS is then completely etched underneath the patch until it is left suspended on the thin dielectric membrane. This configuration provides a localized low dielectric constant region ($\epsilon_r \cong 1$) just around and below the patch.

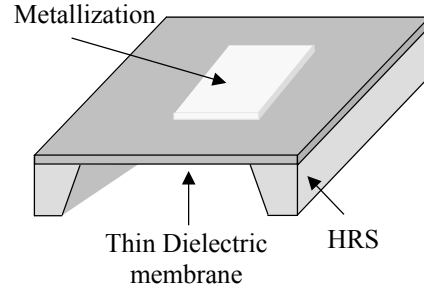


Fig. 1: Process Description

B. Patch Design

The proposed antenna consists of a rectangular patch of dimensions 4x4.8mm². The patch is centered over an air cavity, and held by a 1.4 μm dielectric membrane, as shown in figure 2. The length of the patch corresponds to $\lambda_0/2$, where λ_0 is the wavelength in vacuum. The width of the patch constitutes the radiating slots of the antenna, thus it strongly affects the radiation efficiency of the antenna, as well as the antenna input impedance. The HRS substrate has the following dimensions; thickness 525 μm , length 17mm, and width 17mm (i.e., total substrate area 3cm²).

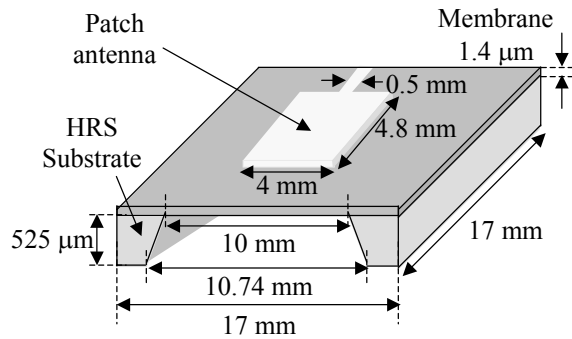


Fig. 2: Patch antenna

The cavity lateral square cross-section length is equal to twice the patch length (i.e. it corresponds to one wavelength). The resultant cavity has lateral dimensions of 10x10mm² in the top plane, and 10.74x10.74mm² in the bottom plane, as shown in figure 2. The effective dielectric constant underneath the antenna is nearly unity. The patch is directly fed at its edge using microstrip line. However, in order to match the high input impedance of the patch, at its feeding point, to the 50 Ω microstrip feed line, a $\lambda/4$ transformer has been designed. The length of this $\lambda/4$ transformer is exactly the length of the line from the patch edge to the point corresponding to the cavity edge. The 50 Ω microstrip feed line over the HRS bulk substrate has the same width as that of the $\lambda/4$ section over the cavity, and consequently there is no sudden change in the line widths.

C. CPW-Microstrip Transition

In order to perform probe measurements of the antenna return loss, a grounded coplanar waveguide (GCPW) to microstrip transition has been designed. The used topology is based on the electromagnetic coupling presented in [6-7]. The transition is simply two 90 $^\circ$ open stubs. The transition configuration and dimensions are shown in figure 3. The dimensions of the CPW line correspond to a characteristic impedance of 50 Ω . The 50 Ω microstrip line width is equal to 0.5mm. The coupling region has a length of 0.7mm,

corresponding to $\lambda_g/4$ at 26 GHz. The transition ends are terminated by open circuits; therefore there is a short circuit at the beginning of the CPW. This will suppress the excitation of Coplanar Microstrip (CPM) Modes in the CPW. The width (0.25mm) and the length (0.7mm) of the 90° open stubs are numerically optimized using HFSS[®] [8].

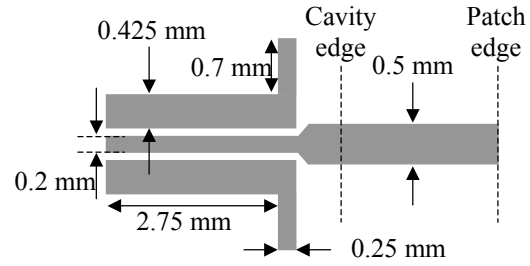


Fig. 3: CPW-Microstrip transition

III. Results and Discussions

The proposed antenna configuration, including the CPW-microstrip transition, has been simulated using the 3D electromagnetic simulator HFSS[®]. A back-to-back transition separated by 2.5mm microstrip line has been designed and simulated. Return loss better than -15dB and insertion loss of -1 dB , in the range 26-28.7 GHz are obtained. The VSWR of the fabricated antenna, including the CPW-microstrip transition, has been measured using HP VNA 8510C and CASCADE probe station. The simulated and measured VSWR is presented in figures 4. Very good agreement between the simulated and measured data is observed. The measured return loss is about -17dB at 26.6 GHz. The measured antenna bandwidth, for $\text{VSWR} \leq 2$, is 4.5%. Figure 5 shows a photo for the fabricated patch antenna mounted on the holder for radiation pattern measurement.

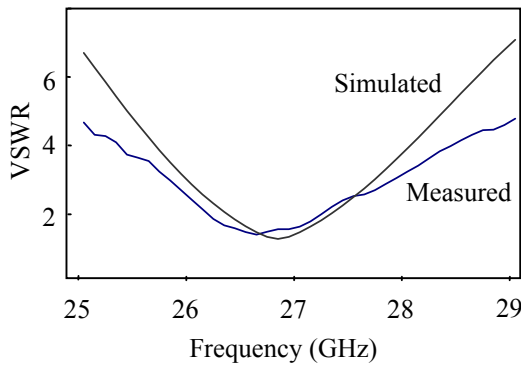


Fig. 4: Measured and simulated VSWR

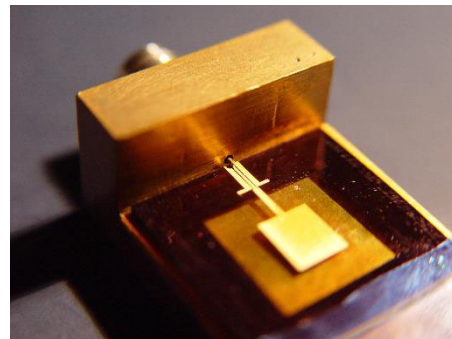


Fig. 5: Photo of the fabricated patch

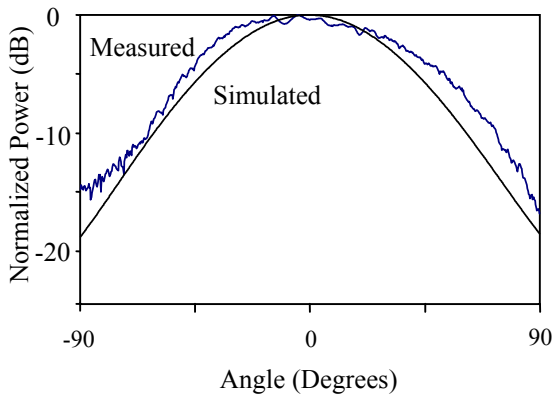


Fig. 6: Measured and simulated H-plane radiation pattern

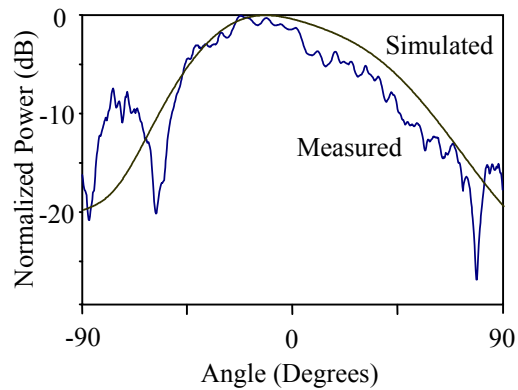


Fig. 7: Measured and simulated E-plane radiation pattern

The radiation pattern measurement has been performed in an anechoic chamber using the network analyzer MVNA 8-350-2 AB Millimeter. The simulated and measured radiation patterns of the antenna in the H- and E-planes are presented in figures 6 and 7, respectively. The H-plane pattern shows symmetrical behavior, and is in very good agreement with the simulated results, with 3-dB beamwidth of approximately 60°. The measured E-plane radiation pattern is tilted of about 10 degrees, and coincides with the simulated results. This is mainly due to the asymmetrical configuration in the E-plane. The sharp minima in the measured E-plane radiation pattern are mainly due to the edges of the antenna holder. The cross polarization level is better than -20dB in the main beam.

IV. Conclusions

A patch antenna operating at 26.6 GHz fabricated using membrane technology over high index substrate is presented. Chemical etching has been used to completely remove the high index substrate underneath the patch, forming an air cavity region with very low dielectric constant ($\epsilon_r \cong 1$). In addition, High Resistivity Silicon (HRS) substrate has been used to reduce the losses due to silicon conductivity. The total substrate area is 3cm²; however this can be additionally reduced if the CPW-microstrip transition is not included. The patch is directly fed using microstrip line. The measured return loss of the patch is in good agreement with the simulated results. The main beam of the antenna has 3-dB beamwidth of 60° in the H-plane, and of 70° in the E-plane. The antenna has a bandwidth of 4.5%, radiation efficiency of 61.7%, and directivity of 7.9dB. The antenna radiation pattern has a cross-polarization level less than -20dB in both the H- and E-planes.

V. Acknowledgment

The authors would like to thank MEMScAP for their financial support of this work, Eric ARNAUD, IRCOM-CREAPE for radiation pattern measurement, and Hubert JALAGEAS, IRCOM for probe measurements.

VI. References

- [1] I. Papapolymerou, R. F. Drayton, and L. P. B. Katehi, "Micromachined patch antenna", *IEEE Trans. Antennas Propagat.*, vol. 46, pp. 275-283, Feb. 1998.
- [2] G. P. Gauthier, J. -P. Raskin, L. P. B. Katehi, and G. M. Rebeiz, "A 94-GHz aperture-coupled micromachined antenna", *IEEE Trans. Antennas Propagat.*, vol. 47, pp. 1761-1765, Dec. 1999.
- [3] M. Zheng, Q. Chen, P. S. Hall, and V. F. Fusco, "Broadband microstrip patch antenna on silicon substrates", *Electron. Lett.*, Oct. 1997.
- [4] G. P. Gauthier, A. Courtay, and G. M. Rebeiz, "Microstrip antennas on synthesized low-dielectric constant substrates", *IEEE Trans. Antennas Propagat.*, vol. 45, pp. 1310-1314, Aug. 1997.
- [5] M. Stotz, H. Haspeklo, and J. Wenger, "Planar millimeter-wave antennas using SiN_x-membranes on GaAs", *IEEE Trans. Antennas Propagat.*, vol. 44, pp. 1593-1595, Sep. 1996.
- [6] J. -P. Raskin, G. Gauthier, L. P. Katehi, and G. M. Rebeiz, "Mode conversion at GCPW-to-microstrip-line transitions", *IEEE Trans. Microwave Theory Tech.*, vol. 48, pp. 158-161, Jan. 2000.
- [7] G. Gauthier, L. P. Katehi, and G. M. Rebeiz, "W-band finite ground coplanar waveguide (FGCPW) to microstrip line transition," in *IEEE-MTT Int. Microwave Symp. Dig.*, Baltimore, MD, June 1998, pp. 107-109.
- [8] Ansoft Corporation, "High Frequency Structure Simulator," version 8.5, June 2002.